ELSEVIER

Cement & Concrete Composites 22 (2000) 259–266

Cement & Concrete Composites

www.elsevier.com/locate/cemconcomp

The nature of C–S–H in model slag-cements

I.G. Richardson *, J.G. Cabrera

Civil Engineering Materials Unit, School of Civil Engineering, University of Leeds, Leeds LS2 9JT, UK

Abstract

Model systems have been used in a large number of studies concerning the chemistry of the hydration of Portland cement. These have most commonly involved tricalcium silicate (C_3S) but C_3S has also been mixed with other components in studies on a variety of composite cements. This paper compares the nature of the C–S–H formed in real slag-cement blends with model systems involving C_3S. The hydration products and microstructural features present in the model and real systems are broadly similar. In both, the morphology of outer product (Op) C–S–H changes from 'fibrillar' to 'foil-like' as the slag content is increased. The Ca/(Si + Al) ratios of inner product (Ip) and Op C–S–H are similar in real slag-cements but are different in the model systems; the difference becomes a little less pronounced at higher slag content. The aluminosilicate anion structures of the C–S–H phases present in the model and real cements are similar with 90% slag but very different with 50% slag.

Keywords: C–S–H; Slag-cement blends; Microanalysis; Microstructure; NMR; TEM

1. Introduction

Many studies concerning the chemistry of the hydration of Portland cement have made use of model systems, most commonly tricalcium silicate (C_3S) since alite, an impure form of C_3S, is Portland cement's major constituent. A nearly amorphous calcium silicate hydrate (C–S–H) is the main binding phase in both hardened C_3S and Portland cement pastes. The nanostructure, morphology, and chemical composition of the C–S–H are very similar in the two systems, although some minor substituents are present when it forms from Portland cement. Taylor [1] has reviewed much of the relevant work. Model systems have also been utilized in studies on a variety of composite cements, for example [2–11]. This paper compares the nature of the C–S–H formed in real slag-cement blends with model systems involving C_3S.

2. Experimental

2.1. Materials

Eight systems were studied; the details are outlined in Table 1. Two commercial blast-furnace slags (SC and VL) (supplied by the Frodingham Cement Company) with different chemical and mineralogical compositions and a synthetic slag-glass (AG) were used; chemical data for the glassy phase present in the slags and fineness data are given in Table 2. Powder X-ray diffraction showed that the commercial slags were >95% glassy. The same slags have been used in other work involving alkali activation [12,13]. The tricalcium silicate (C_3S) used in the work was prepared by the method of Groves et al. [14]. Two Portland cements were used: an ordinary Portland cement (OPC) [15], and a white Portland cement (WPC) (from the Aalborg Company; Bogue composition (wt%) 65% C_3S, 22% C_2S, 4% C_3A, 1% C_4AF). The latter was needed for the NMR work because of its low-Fe content; the presence of paramagnetic ions causes peak broadening in NMR.

2.2. Specimen preparation and experimental details

The required amounts of solids were mixed with deionized water, placed in plastic tubes and sealed in plastic bags before placing in a cure bath. Details of sample

* Corresponding author. Tel.: +44-0113-233-2331; fax: +44-0113-233-2265.

E-mail address: i.g.richardson@leeds.ac.uk (I.G. Richardson).

0958-9465/00/$ - see front matter
PII: S0958-9465(00)00022-6

Table 1
Details of the systems studied

Slag	%	Cement	%	W/S	Temperature (°C)
–	–	OPC	100	0.4	20
–	–	C_3S	100	0.4	20
VL	50	WPC	50	0.4	25
VL	90	WPC	10	0.4	25
SC	50	C_3S	50	0.4	20
SC	90	C_3S	10	0.4	20
AG	50	C_3S	50	0.4	20
AG	90	C_3S	10	0.4	20

Table 2
Granulated blast-furnace slags: glass composition (determined by wavelength dispersive X-ray analysis) and fineness data[a]

	SC	VL	AG
Ca/Si	1.10	1.21	1.09
Al/Si	0.36	0.40	0.33
Mg/Si	0.32	0.44	0.30
n	0.99	0.89	0.99
x_0 μm	22.9	17.5	24.0
Median	16.9	9.7	18.0

[a] n and x_0 represent the particle size distribution (Rosin–Rammler constants): n is a measure of breadth of distribution (higher $n \rightarrow$ narrower); x_0 is a measure of average size (36.8% of particles are $> x_0$ μm).

preparation and experimental procedures for analytical transmission electron microscopy (TEM) are given elsewhere [14,15]. Specimens for nuclear magnetic resonance (NMR) spectroscopy were ground to a powder (not dried) and packed into zirconia rotors. The ^{29}Si NMR spectra were acquired using Bruker MSL-200 (magnetic field 4.7 T; operating frequency of 39.76 MHz for ^{29}Si) and MSL-300 (magnetic field 7.1 T; operating frequency of 59.62 MHz for ^{29}Si) spectrometers. The single pulse (SP) spectra were acquired over 4000–42000 scans using flip angles (30–45°) and pulse recycle delays (2–20 s) sufficient to minimize saturation effects. For the ^{1}H–^{29}Si cross-polarization (CP) experiments, the Hartmann–Hahn condition was set using kaolinite [16]. ^{29}Si chemical shifts are given relative to tetramethylsilane (TMS) at 0 ppm, with kaolinite used as an external standard at −91.2 ppm. The spectra were iteratively fitted to Voigt line shapes using the software Igor [17] with additional macros written by Brough [18]. A detailed account of the deconvolution procedure is given elsewhere [13].

3. Results and discussion

3.1. Hydration products and microstructure

The hydration products and microstructural features present in the model systems are broadly similar to those in the real cements, and can be classified as either 'inner', forming within the boundaries of the original anhydrous grains – whether cement or slag – or 'outer', forming in the originally water-filled spaces.

The main outer hydration products in all the systems are C–S–H and $Ca(OH)_2$ with AFm present in the white cement-slag blends. In all cases, the C–S–H is nearly amorphous and the $Ca(OH)_2$ occurs as large plates and is more abundant in the cement- or C_3S-rich systems. Inner product (Ip) and outer product (Op) C–S–H are morphologically distinct from one another. Ip in larger grains generally has a dense homogeneous morphology with only very fine porosity. Slag-derived Ip with a fine dense morphology is shown in the bottom left of Fig. 1 (90% slag 10% C_3S blend, in this case hydrated for 18 months). The morphology of Op C–S–H in the model systems varies with chemical composition in the same way that it does in the real Portland cement-slag blends: at high-Ca/Si ratio it has a fibrillar morphology which gradually changes to foil-like with a reduction in Ca/Si ratio (see [19] for a discussion regarding the morphology of Op C–S–H). Op C–S–H with foil-like morphology is shown in the top right of Fig. 1: this morphology is typical of high-slag- or, indeed, high-pozzolan-cements and is likely to be largely responsible for the improved durability performance possible with such systems. To illustrate the similarity, Fig. 2 shows the fine foil-like Op C–S–H in a 90% slag 10% Portland cement blend. Fig. 3

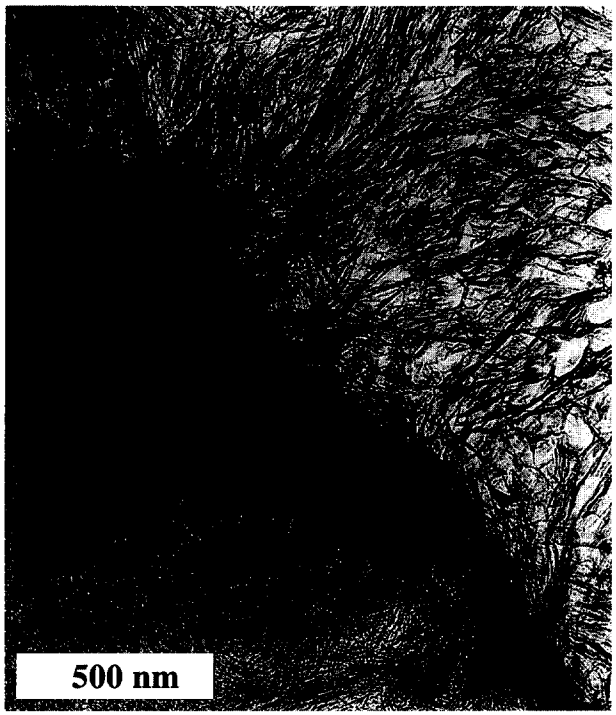

Fig. 1. Transmission electron micrograph showing a region of slag-derived Ip (bottom left) with fine dense morphology and foil-like Op C–S–H in a 90% slag 10% C_3S blend hydrated for 18 months at 20°C.

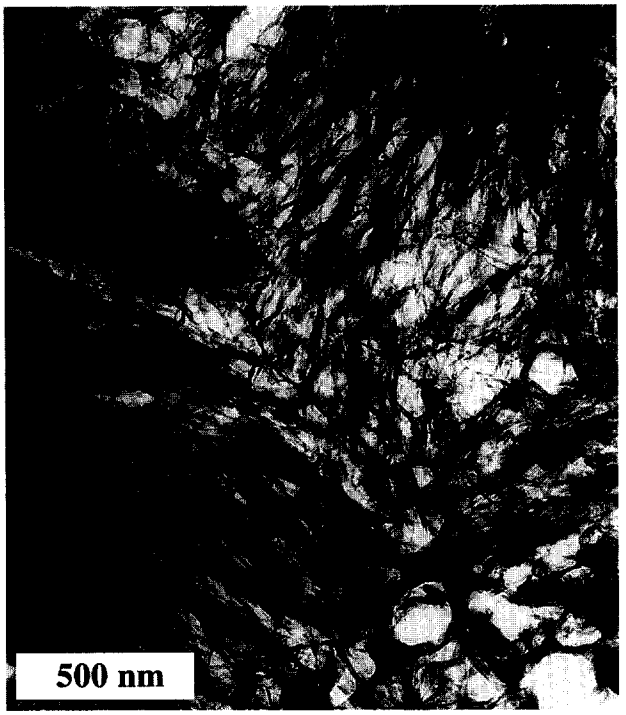

Fig. 2. Transmission electron micrograph showing fine foil-like Op C–S–H in a mature 90% slag 10% Portland cement blend.

shows two other types of inner product: in the top right is a region of Ip from a C_3S grain, which, unlike that from the slag in Fig. 1, has suffered severe damage in the electron beam (the pore structure has coarsened); in the centre-left of the micrograph is a good example of a small fully hydrated slag grain possessing the dense outer rim and less-dense interior which are characteristic features of small fully hydrated grains in general [19].

As noted, Op C–S–H present in low-slag systems is fibrillar rather than foil-like in character. This is illustrated in Fig. 4, which shows coarse fibrillar Op C–S–H between two regions of synthetic slag-glass Ip, and in Fig. 5, which again shows coarse fibrillar Op C–S–H, but in this case surrounding a partially hydrated C_3S grain. As with the 90% slag systems, it is again notable that the C_3S-derived Ip C–S–H has suffered extensive damage (coarsening of porosity) in the electron beam, in contrast to the slag-Ip which is much more stable.

Slag-glass Ip can in all cases be considered to be an intimate mixture of C–S–H and a Mg, Al hydroxide type phase.

3.2. Chemical composition of the C–S–H

The composition of C–S–H present in hardened Portland cement pastes is very similar to that present in C_3S pastes but contains a small amount of aluminium substituted for silicon. The average Ca/Si ratio in both is always around 1.7–1.8 [15] and the compositions of Ip

Fig. 3. Transmission electron micrograph showing two types of inner product in a 90% slag 10% C_3S blend hydrated for 18 months at 20°C: Ip from a C_3S grain (top right) and a small fully hydrated slag grain (centre-left).

and Op C–S–H are similar. This is illustrated in Fig. 6 which shows Ca/Si ratio frequency histograms for C–S–H present in C_3S and Portland cement pastes (in these cases hydrated for three years at 20°C). These data are from analyses in the TEM of C–S–H free of admixture with other phases [15]. In slag-cement blends, Ip C–S–H from cement grains has a Ca/(Si + Al) ratio similar to Op C–S–H. This is illustrated in Fig. 7 for a 50% slag 50% WPC hydrated for three weeks. This similarity is common in slag-Portland cement blends over a wide range of slag loading [20]. The situation is different, however, in the model slag-cement blends – whether C_3S with the synthetic slag-glass or a commercial slag – where the Ca/(Si + Al) ratio is higher for Op C–S–H than for C_3S-derived Ip C–S–H, Fig. 8. Indeed, the Ca/(Si + Al) ratio of Op C–S–H is higher in blends containing 50% C_3S than in those with 50% Portland cement. This is illustrated in Fig. 9 for three months hydration. Although the overall Ca/(Si + Al) ratio of C–S–H is much lower in blends with higher slag loading, there is still a difference between C_3S-Ip and Op C–S–H composition. This is illustrated in Fig. 10 for a 90% slag 10% C_3S blend hydrated for 18 months.

Fig. 4. Transmission electron micrograph showing coarse fibrillar Op C–S–H between two regions of synthetic slag-glass Ip in a 50% C_3S 50% synthetic slag-glass hydrated for 1 month.

Fig. 5. Transmission electron micrograph showing coarse fibrillar Op C–S–H surrounding a partially hydrated C_3S grain in a 50% C_3S 50% synthetic slag-glass hydrated for 1 month.

3.3. Aluminosilicate anion structure

To facilitate comparison between real and model cements, Figs. 11 and 12 show ^{29}Si NMR spectra for slag-WPC blends activated with water (modified from [13]). Fig. 11 (bottom) shows the SP NMR spectrum for a 50% slag 50% WPC blend hydrated for three weeks. The sharp peak at −71.3 ppm is due to unreacted belite (isolated silicate tetrahedra, Q^0). The broader peaks between around −79 and −85 ppm, which are present on both the SP and CP spectra are due to silicate groups in the C–S–H (the belite peak and a very broad peak centred on around −73 ppm due to unreacted slag-glass are absent from the CP spectrum because the CP experiment probes only the hydrate phases). Using information derived from the deconvolution of better-resolved spectra produced by alkali-activation of the blends, Richardson and Groves [13] showed that the SP spectrum could be deconvoluted satisfactorily using three C–S–H peaks at −78.9 (chain-end groups, Q^1), and −81.5 and −84.5 ppm (middle-chain groups, Q^2(1Al) and Q^2(0Al), respectively). The Al/Si ratio for the C–S–H calculated from the peak areas was in excellent agreement with the value determined directly by analysis in the TEM of C–S–H free of admixture with other phases. Fig. 12 shows the SP (bottom) and CP spectra for a water activated 90% slag 10% WPC blend, again hydrated for three weeks. The SP spectrum could be fitted with Q^1, Q^2(1Al) and Q^2(0Al) peaks at −79.0, −81.1, and −84.5 ppm, respectively [13]. Again the Al/Si ratio calculated from the peak areas was in excellent agreement with the value from TEM. Figs. 13 and 14 show SP (bottom) and CP spectra for C_3S-synthetic slag-glass blends (hydrated for 2 weeks) with 50% and 90% slag-glass, respectively. In the SP spectra, the sharp peaks between −69 and −75 ppm are due to unreacted C_3S and there is a broad peak centred on around −75 ppm due to unreacted slag-glass. The spectra for the 50% C_3S/slag-glass blend, Fig. 13, are very different to those for the 50% Portland cement/slag blend, Fig. 11. The C–S–H in the former has a much shorter average aluminosilicate chain length than the latter, which is consistent with its higher average Ca/Si ratio. The spectra for the C_3S-containing blend are also consistent with the TEM analyses, which indicate only minor substitution of Al for Si; the synthetic slag-glass is not

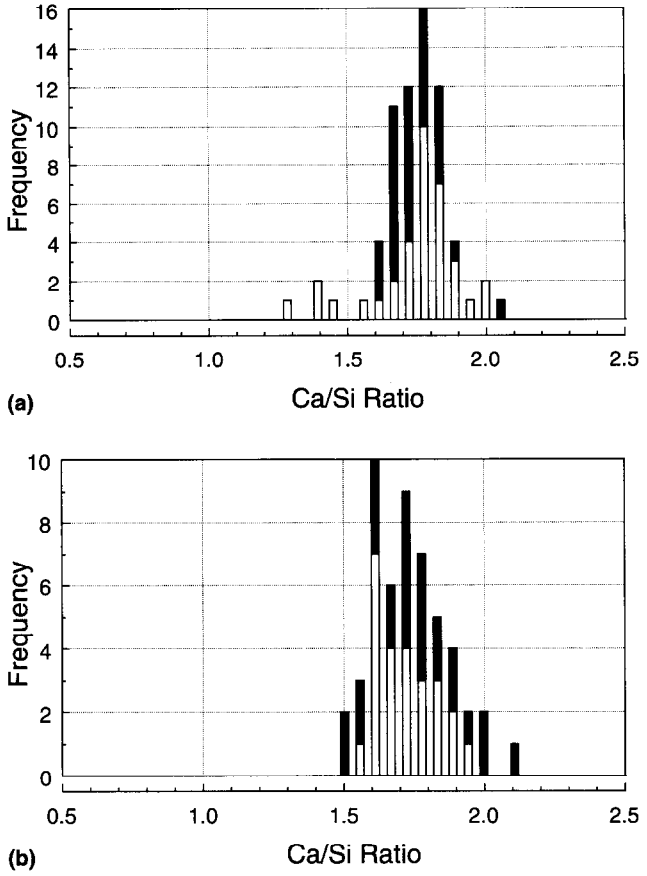

Fig. 6. Ca/Si ratio frequency histogram for C–S–H in (a) C_3S and (b) Portland cement pastes hydrated for three years (TEM microanalyses of C–S–H free of admixture with other phases). Ip (■) Op (□).

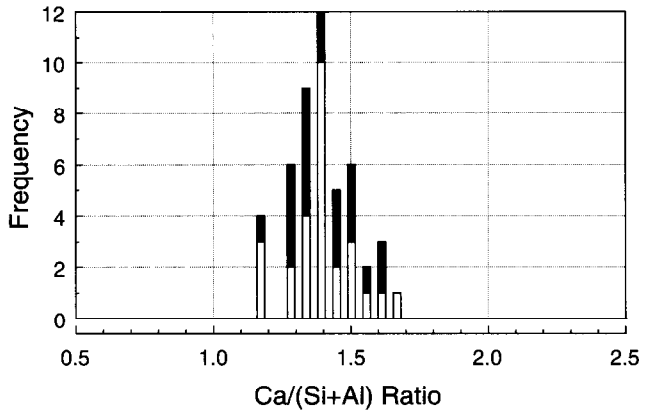

Fig. 7. Ca/(Si + Al) ratio frequency histogram for C–S–H in a 50% slag 50% WPC paste hydrated for three weeks (TEM microanalyses of C–S–H free of admixture with other phases). Ip (■) Op (□).

well-reacted after two weeks hydration. On more prolonged curing, the average length of the aluminosilicate anions increases in both the real (compare Fig. 11 with Fig. 14(a) of [19]) and model systems (compare Fig. 13 with Fig. 15) but there is still only modest substitution of Al for Si in the C_3S-containing system.

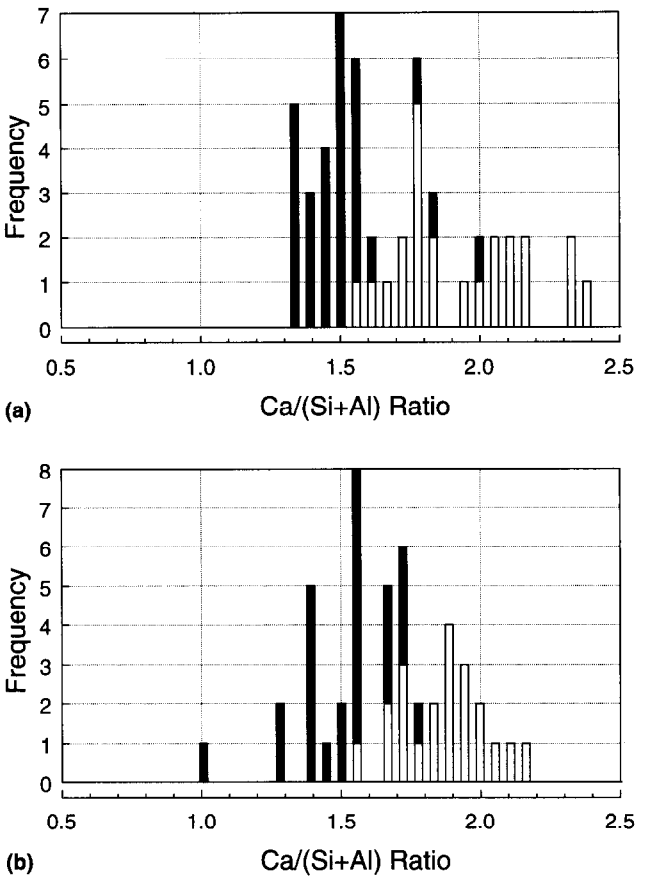

Fig. 8. Ca/(Si + Al) ratio frequency histograms for C–S–H in (a) 50% slag 50% C_3S and (b) 50% synthetic slag-glass 50% C_3S pastes both hydrated for three months (TEM microanalyses of C S H free of admixture with other phases). Ip (■) Op (□).

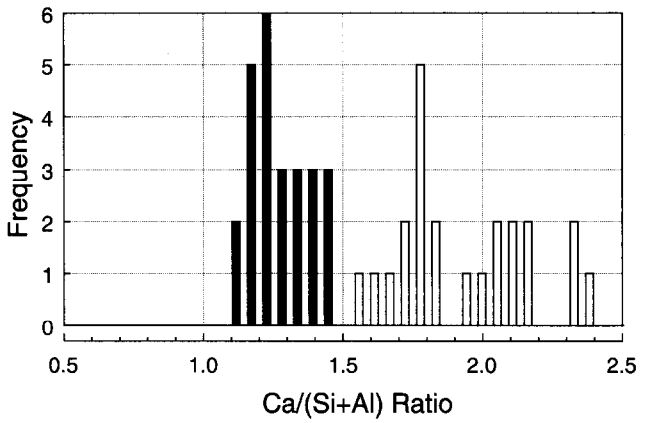

Fig. 9. Ca/(Si + Al) ratio frequency histogram for Op C–S–H in 50% slag 50% ordinary Portland cement and 50% slag 50% C_3S pastes hydrated for three months (TEM microanalyses of C–S–H free of admixture with other phases). Ordinary Portland cement (■) C_3S (□).

In contrast to the systems containing 50% slag, the aluminosilicate anion structures of the C–S–H present in

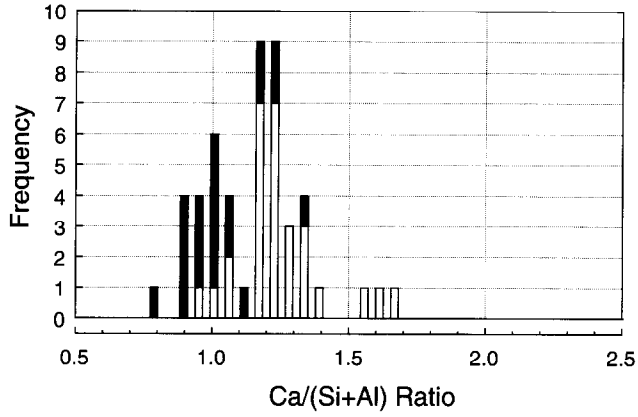

Fig. 10. Ca/(Si + Al) ratio frequency histogram for C–S–H in a 90% slag 10% C_3S hydrated for 18 months (TEM microanalyses of C–S–H free of admixture with other phases). Ip (■) Op (□).

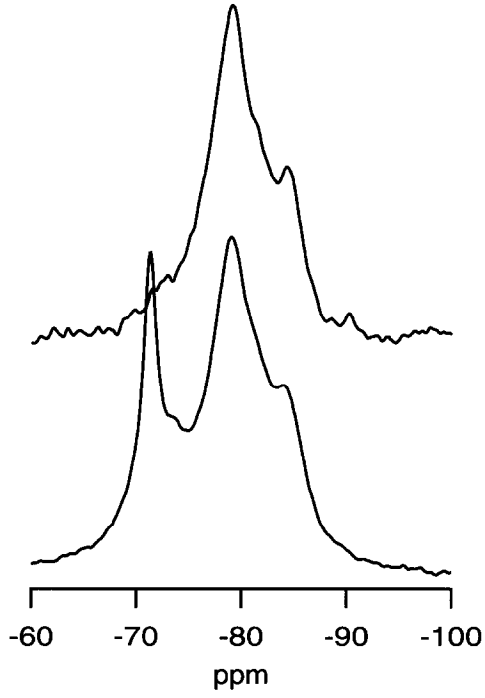

Fig. 11. ^{29}Si SP (bottom) and ^{1}H–^{29}Si CP MAS NMR spectra of a water-activated 50% WPC 50% slag blend hydrated for three weeks at 25°C; W/S = 0.4.

the real and model systems with 90% are quite similar; for example, compare Figs. 12 and 14.

4. Conclusions

1. The hydration products and microstructural features present in model and real slag-cements are broadly similar.

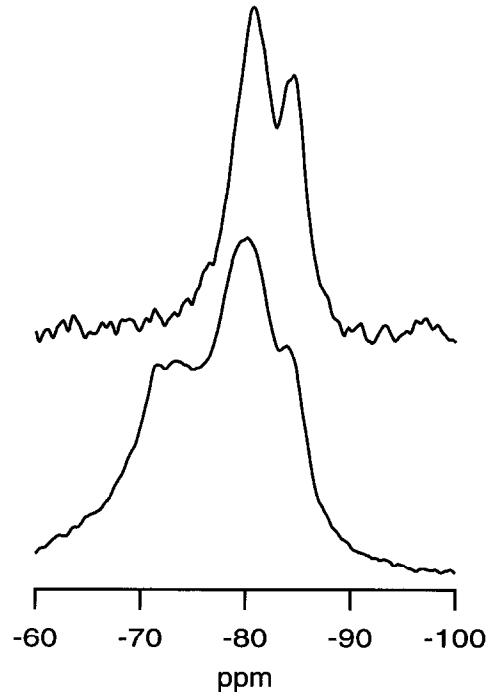

Fig. 12. ^{29}Si SP (bottom) and ^{1}H–^{29}Si CP MAS NMR spectra of a water-activated 10% WPC 90% slag blend hydrated for three weeks at 25°C; W/S = 0.4.

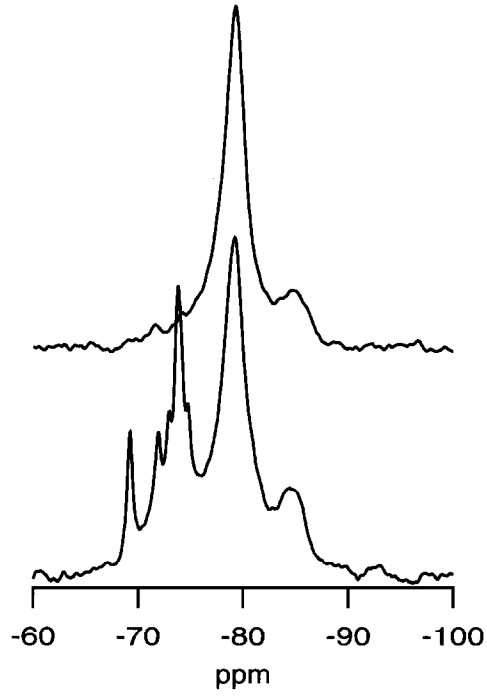

Fig. 13. ^{29}Si SP (bottom) and ^{1}H–^{29}Si CP MAS NMR spectra of a water-activated 50% C_3S 50% synthetic slag-glass hydrated for two weeks at 20°C; W/S = 0.4.

2. In both model and real systems, the morphology of Op C–S–H changes from fibrillar to foil-like as the slag content is increased.

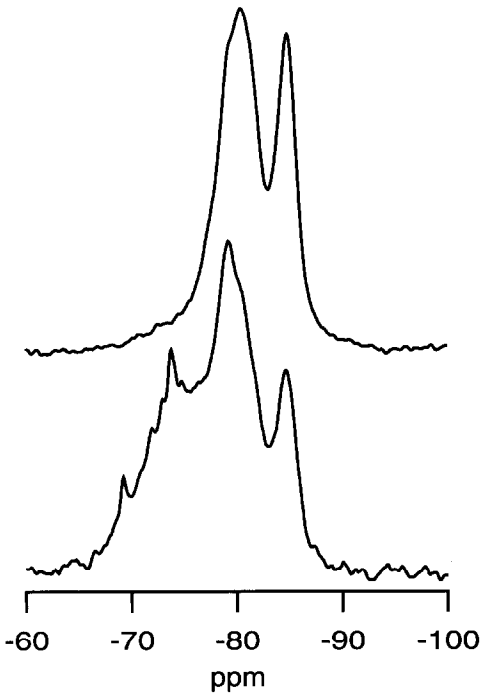

Fig. 14. ^{29}Si SP (bottom) and ^{1}H–^{29}Si CP MAS NMR spectra of a water-activated 10% C_3S 90% synthetic slag-glass hydrated for two weeks at 20°C; W/S = 0.4.

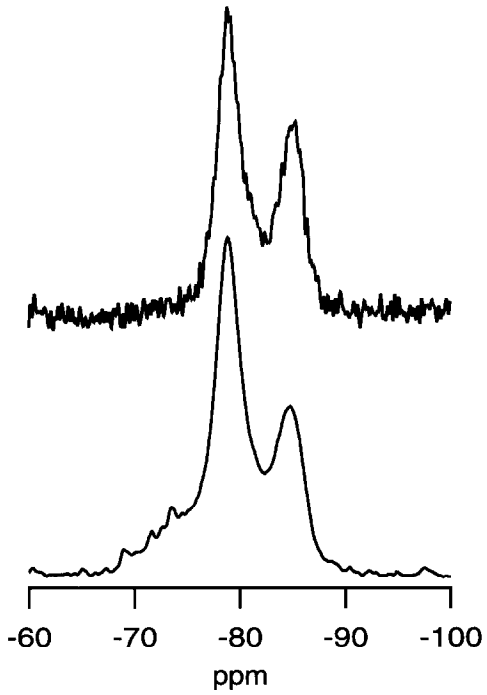

Fig. 15. ^{29}Si SP (bottom) and ^{1}H–^{29}Si CP MAS NMR spectra of a water-activated 50% C_3S 50% synthetic slag-glass hydrated for five months at 20°C; W/S = 0.4.

3. The Ca/(Si + Al) ratios of Ip and Op C–S–H are similar in real slag-cements but are different in the model systems; the difference becomes a little less pronounced at higher slag content.
4. The aluminosilicate anion structures of the C–S–H phases present in the model and real cements are similar with 90% slag but very different with 50% slag.

Acknowledgements

Thanks are due to the Engineering and Physical Sciences Research Council for funding under Grant Nos. GR/H64972 and GR/K65478, to Dr. Geoff. Groves for encouragement and support, and to Prof. Neville Boden (SOMS Centre, University of Leeds) and Prof. Chris Dobson FRS (Inorganic Chemistry Laboratory, University of Oxford) for provision of the NMR facilities.

References

[1] Taylor HFW. Cement Chemistry. 2nd ed. London: Thomas Telford, 1997.
[2] Ogawa K, Uchikawa H, Takemoto K, Yasui I. The mechanism of the hydration in the C_3S-pozzolana. Cem Concr Res 1980;10:683–96.
[3] Mohan K, Taylor HFW. Effects of flyash incorporation in cement and concrete. Mater Res Soc 1981:54.
[4] Uchikawa H, Furuta R. Hydration of C_3S-pozzolana paste estimated by trimethylsilylation. Cem Concr Res 1981;11:65–78.
[5] Massazza F, Testolin M. Trimethylsilylation in the study of pozzolana-containing pastes. Il Cemento 1983;80:49–62.
[6] Uchikawa H. Effect of blending components on hydration and structure formation. In: Eighth International Congress Chem Cem, vol. 1, 1986, p. 249–80.
[7] Wu Z-Q, Young JF. The hydration of tricalcium silicate in the presence of colloidal silica. J Mater Sci 1984;19:3477–86.
[8] Dobson CM, Goberdhan GCD, Ramsay JDF, Rodger SA. ^{29}Si MAS NMR study of the hydration of tricalcium silicate in the presence of finely divided silica. J Mater Sci 1988;23:4108–14.
[9] Rodger SA, Groves GW. The microstructure of tricalcium silicate/pulverized fuel ash blended cement pastes. Adv Cem Res 1988;1(2):84–91.
[10] Richardson IG, Wilding CR, Dickson MJ. The hydration of blast-furnace slag cements. Adv Cem Res 1989;2:147–57.
[11] Brough AR, Dobson CM, Richardson IG, Groves GW. A study of the pozzolanic reaction by solid-state ^{29}Si nuclear magnetic resonance using selective isotopic enrichment. J Mater Sci 1995;30:1671–8.
[12] Richardson IG. The structure of C–S–H in hardened slag cement pastes. In: 10th International Congress Chem Cem, vol. 2, 1997, p. 2ii068, 8.
[13] Richardson IG, Groves GW. The structure of the calcium silicate hydrate phases present in hardened pastes of white Portland cement/blast-furnace slag blends. J Mater Sci 1997;32:4793–802.
[14] Groves GW, LeSueur PJ, Sinclair W. Transmission electron microscopy and microanalytical studies of ion-beam-thinned sections of tricalcium silicate paste. J Am Ceram Soc 1986;69:353–6.

[15] Richardson IG, Groves GW. The microstructure and microanalysis of hardened ordinary Portland cement pastes. J Mater Sci 1993;28:265–77.
[16] Rocha J, Klinowski J. Kaolinite as a convenient standard for setting the Hartmann–Hahn match for ^{29}Si CP MAS NMR of silicates. J Magn Reson 1990;90(3):567–8.
[17] WaveMetrics, Inc., Igor (1992) and Igor Pro (1996), Lake Oswego, Oregon, 97035, USA.
[18] Brough AR. D. Phil. Thesis, University of Oxford, 1993.
[19] Richardson IG. The nature of C–S–H in hardened cements. Cem Concr Res 1999;29:1131–47.
[20] Richardson IG, Groves GW. The microstructure and microanalysis of hardened cement pastes involving ground granulated blast-furnace slag. J Mater Sci 1992;27:6204–12.